Molecular Therapy
Original Article

Gene Therapy Corrects Brain and Behavioral Pathologies in CLN6-Batten Disease

Jacob T. Cain,[1,8] Shibi Likhite,[2,8] Katherine A. White,[1,8] Derek J. Timm,[1] Samantha S. Davis,[1] Tyler B. Johnson,[1] Cassandra N. Dennys-Rivers,[2] Federica Rinaldi,[2] Dario Motti,[2] Sarah Corcoran,[2] Pablo Morales,[3] Christopher Pierson,[2] Stephanie M. Hughes,[4] Stella Y. Lee,[5] Brian K. Kaspar,[6,9] Kathrin Meyer,[2,9] and Jill M. Weimer[1,7,9]

[1]Pediatrics and Rare Diseases Group, Sanford Research, Sioux Falls, SD 57104, USA; [2]The Research Institute at Nationwide Children's Hospital, Columbus, OH 43205, USA; [3]The Mannheimer Foundation, Inc., Homestead, FL 33034, USA; [4]Department of Biochemistry, School of Biomedical Sciences, Brain Health Research Centre, University of Otago, Dunedin 9016, New Zealand; [5]Division of Biology, Kansas State University, Manhattan, KS 66506, USA; [6]AveXis Inc., Bannockburn, IL 60015, USA; [7]Department of Pediatrics, Sanford School of Medicine, University of South Dakota, Sioux Falls, SD 57069, USA

CLN6-Batten disease, a form of neuronal ceroid lipofuscinosis is a rare lysosomal storage disorder presenting with gradual declines in motor, visual, and cognitive abilities and early death by 12–15 years of age. We developed a self-complementary adeno-associated virus serotype 9 (scAAV9) vector expressing the human *CLN6* gene under the control of a chicken β-actin (CB) hybrid promoter. Intrathecal delivery of scAAV9.CB.hCLN6 into the cerebrospinal fluid (CSF) of the lumbar spinal cord of 4-year-old non-human primates was safe, well tolerated, and led to efficient targeting throughout the brain and spinal cord. A single intracerebroventricular (i.c.v.) injection at postnatal day 1 in *Cln6* mutant mice delivered scAAV9.CB.CLN6 directly into the CSF, and it prevented or drastically reduced all of the pathological hallmarks of Batten disease. Moreover, there were significant improvements in motor performance, learning and memory deficits, and survival in treated *Cln6* mutant mice, extending survival from 15 months of age (untreated) to beyond 21 months of age (treated). Additionally, many parameters were similar to wild-type counterparts throughout the lifespan of the treated mice.

INTRODUCTION

Batten disease (also called neuronal ceroid lipofuscinoses [NCLs]) comprises a family of rare, genetic, lysosomal storage disorders that are universally fatal. This family of diseases is caused by mutations in one of approximately 13 known ceroid-lipofuscinosis neuronal (*CLN*)-related genes.[1] Collectively, Batten disease is the most prevalent cause of neurodegenerative disease in children, with an incidence of 2–4/100,000 live births.[2,3] Common disease symptomology and pathology in this family of diseases involves progressive visual, motor, and mental deterioration, with shortened lifespan.

At the cellular level, lysosmal dysfunction results in the accumulation of lipofuscin, an autoflourescent fatty material comprising multiple accumulates, including mitochondrial ATP synthase subunit C.[4] Batten disease primarily manifests in the CNS, where the progressive death of neurons contributes to the clinical signs and symptoms. Disease age of onset and disease progression vary considerably depending on the genetic variant of the disease. Here, we focus on CLN6-Batten disease, which can occur as two different forms: variant late-infantile (vLINCL), the more common form, and adult-onset NCL (also called type A Kufs disease).[5,6] With vLINCL (referred to here as CLN6-Batten disease), age of onset is between 18 months and 6 years and death typically occurs by age 12–15. CLN6-Batten disease initially presents as impaired language and delayed motorand cognitive development in early childhood, with most patients being wheelchair bound within 4 years of disease onset.[7] The disease progresses to include visual loss, severe motor deficits, recurrent seizures, dementia, and other neurodegenerative symptoms.

CLN6 is a 311-amino acid protein with seven predicted transmembrane domains, and it is predominately localized to the endoplasmic reticulum.[8,9] As with other CLN proteins, its exact function remains unclear; however, it has been implicated in intracellular trafficking and lysosomal function.[10–12] There are currently over 70 characterized disease-causing mutations in *CLN6*,[13] with most of these mutations leading to either a complete loss of CLN6 protein or production of truncated CLN6 protein products that are thought to be highly unstable and/or non-functional.[14] Several naturally occurring animal models of CLN6-Batten disease have been described;[15] these include sheep,[16,17] canine,[18] and mouse models.[19] The spontaneous mutation found in the $Cln6^{nclf}$ mouse model, the model used in this study, recapitulates many of the pathological and behavioral aspects of the disease.[20] The $Cln6^{nclf}$ mice contain an insertion of an additional cysteine (c.307insC, frameshift after P102), resulting in a premature stop

Received 13 November 2018; accepted 25 June 2019;
https://doi.org/10.1016/j.ymthe.2019.06.015.

[8]These authors contributed equally to this work.

[9]These authors contributed equally to this work.

Correspondence: Jill M. Weimer, Pediatrics and Rare Diseases Group, Sanford Research, 2301 E. 60th St. N., Sioux Falls, SD 57104, USA.
E-mail: jill.weimer@sanfordhealth.org

codon[21] that is homologous to a mutation commonly found in CLN6-Batten disease patients.[9]

Given that there is no effective cure for CLN6-Batten disease, we used the *Cln6*^{nclf} mouse model to test the efficacy of introducing functional human *CLN6* via adeno-associated virus (AAV)-mediated gene therapy. Our pre-clinical results suggest that use of AAV-serotype 9 allows efficient expression of the human CLN6 protein throughout the CNS, where the most impacted cells are located. To evaluate safety of the treatment in a larger animal model, we dosed three 4-year-old cynomolgus macaques with self-complementary AAV serotype 9 (scAAV9).chicken β-actin (CB).CLN6 by intrathecal lumbar cerebrospinal fluid (CSF) injection, and we monitored them for up to 6 months post-injection. No adverse effects or pathology were observed, while high levels of transgene expression were found throughout the brain and spinal cord of all animals. A single, post-natal intracerebroventricular (i.c.v.) injection of scAAV9.CB.CLN6 into the CSF of mice induced persistent expression of the transgene *in vivo* in *Cln6*^{nclf} mice. Administration of scAAV9.CB.CLN6 prevented the classic hallmarks of the disease, including accumulation of autofluorescent storage material and ATP synthase subunit C, reactive gliosis, and loss of dendritic spines. Importantly, this gene therapy treatment led to extensive functional benefits, as it prevented many of the motor, memory and learning, and survival deficits of the *Cln6*^{nclf} mice. These results strongly underline the therapeutic potential of CSF-delivered scAAV9.CB.CLN6 for the treatment of CLN6-Batten disease.

RESULTS

hCLN6 Transcript and Protein Expressions Are Sustained through 18 Months of Age

To express human *CLN6* (*hCLN6*), we designed an scAAV9 viral vector with the *hCLN6* gene under control of the CB hybrid promoter, notated as scAAV9.CB.CLN6 (Figure S1A). This specific vector was chosen based on its CNS transduction efficiency and its proven safety in human subjects, as documented in a current phase I clinical trial for infants with type I spinal muscular atrophy.[22] After cloning, transgene mRNA and protein expressions were verified *in vitro* in HEK293 cells (Figure S1B). Given the overarching concern in the Batten disease research community that overexpression of NCL proteins (including CLN6, CLN3, and CLN8) might be toxic to cells, we assessed this possibility by overexpressing hCLN6 in excitatory projection neurons of the cortical plate using a non-viral delivery method.

Cortical neurons were targeted using *in utero* i.c.v. electroporation of embryonic day 15.5 animals. Animals were electroporated with either scAAV9.CB.CLN6 or scAAV9.CB.GFP plasmids (1 ug/animal) and sacrificed at post-natal day 14 (P14), and the cellular trafficking of hCLN6 was examined. The additional GFP vector was used to visualize the distribution of scAAV9.CB.CLN6 in comparison to a non-NCL-expressing vector, indicating no abnormalities with hCLN6 distribution in cortical neurons *in vivo* (Figure S1C). Additionally, hCLN6 appeared to be properly trafficked in cortical neurons, and both vectors demonstrated robust expression in the cerebral cortex *in vivo*, indicating that overexpression of hCLN6 in cortical neurons alone does not appear to be detrimental to cells (Figure S1C).

The efficacy of *CLN6* gene delivery following a single i.c.v. injection of scAAV9.CB.CLN6 (5×10^{10} vg/animal) into the CSF at P1 was determined in male and female *Cln6*^{nclf} mice. Extensive details on animal usage and study design can be found in the Materials and Methods. These mice are a naturally occurring mouse model of CLN6-Batten disease, displaying major disease hallmarks found in human patients.[19,20] Examination of *hCLN6* expression by RT-PCR at 2, 6, and 18 months post-injection demonstrated sustained, robust *hCLN6* expression in the cortex of scAAV9.CB.CLN6-injected *Cln6*^{nclf} mice compared to PBS-injected controls (Figure 1A; Figure S2A), similar to previously reported scAAV9-CB-GFP expression levels.[23–25] To examine the regional distribution of transgene expression, a modified *in situ* hybridization method called RNAScope was used to visualize *hCLN6* transcript. scAAV9.CB.CLN6-injected mutant mice (i.c.v., P1, 5×10^{10} vg/animal) maintained a widespread expression of *hCLN6* throughout many regions of the brain at 2, 6, and 18 months, including the somatosensory cortex and ventral posteromedial (VPM)/ventral posterolateral (VPL) nuclei of the thalamus, two regions that have been shown to be affected earliest in the disease progression of the *Cln6*^{nclf} mice (Figure 1B; Figures S2B and S3A).

To examine the expression of hCLN6 protein within the CNS, immunoblotting of cortical brain lysates harvested from scAAV9.CB.CLN6-injected *Cln6*^{nclf} mice (i.c.v., P1, 5×10^{10} vg/animal) and PBS-injected controls was performed using anti-hCLN6 antibodies. Similar to what was seen with RNA expression, robust hCLN6 protein expression was seen throughout the CNS at 2, 6, and 18 months post-injection (Figure 1A; Figure S2A). Furthermore, immunolabeling of brain tissue using anti-hCLN6 antibodies confirmed the expression throughout the brain of scAAV9.CB.CLN6-treated *Cln6*^{nclf} mice, particularly in the VPM/VPL and somatosensory cortex (Figure 1C; Figures S2B, S3B, and S4). Together, these findings demonstrate that CSF delivery of scAAV9.CB.CLN6 via i.c.v. injection is able to stably produce *hCLN6* transcript and protein in disease-relevant regions of the CNS.

Sustained Expression of hCLN6 Prevents Classic CLN6-Batten Disease Pathology in the Brain

Although the pathogenicity of autofluorescent storage material (ASM) is not entirely understood, the accumulation of ASM is a hallmark of all forms of Batten disease. At 2, 6, and 18 months post-treatment, *Cln6*^{nclf} mice injected with scAAV9.CB.CLN6 (i.c.v., P1, 5×10^{10} vg/animal) had a reduced accumulation of ASM within the VPM/VPL nuclei of the thalamus and somatosensory cortex of the brain compared to PBS-injected mice (Figure 2A; Figure S2C). Because PBS-treated *Cln6*^{nclf} mice die by 15 months of age (as demonstrated in Figure 5D), moribund 12- to 14-month-old PBS-treated *Cln6*^{nclf} mice were used as a comparison to 18-month-old scAAV9.CB.CLN6-treated *Cln6*^{nclf} mice. Notably, the amount of ASM accumulation in these 18-month-old scAAV9.CB.CLN6-injected *Cln6*^{nclf} mice was comparable to the age-matched untreated wild-type mice. One primary constituent of

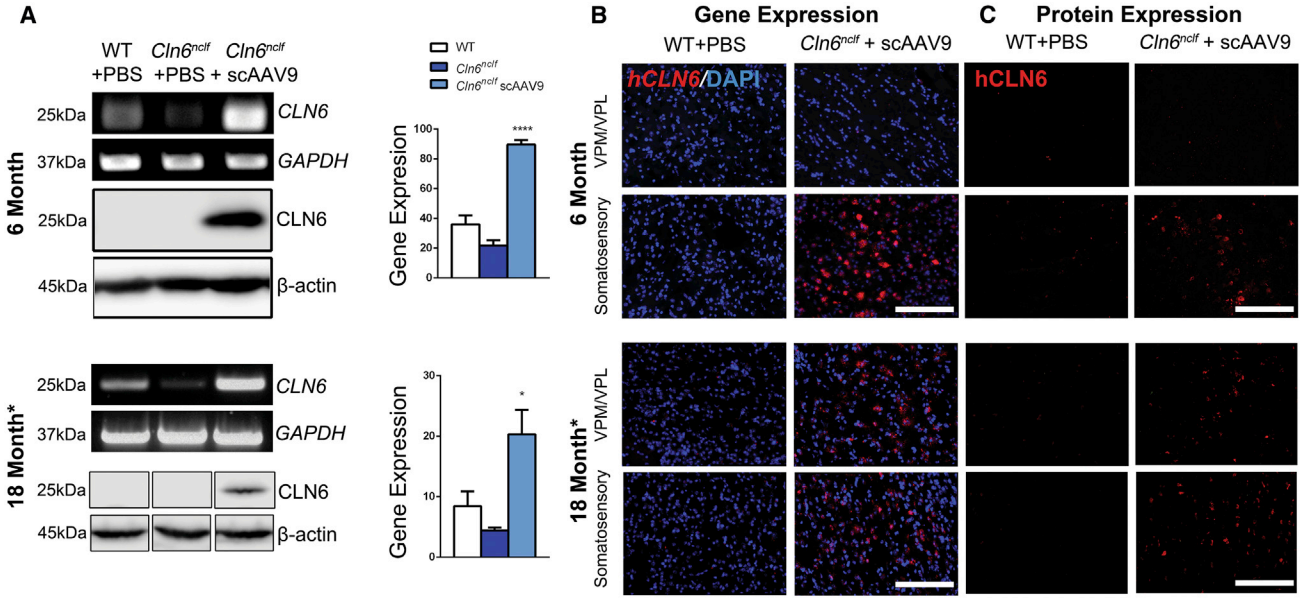

Figure 1. Widespread RNA and Protein Expressions of hCLN6 throughout the CNS of CLN6-Batten Disease Mouse Model in 6- and 18-Month-Old Animals following Single i.c.v. Injection

(A) Top gels and graphs: representative RT-PCR gels and densitometry (normalized to *GAPDH*) show increased *hCLN6* gene expression (25 kDa) following a single i.c.v. injection of scAAV9.CB.CLN6 (5×10^{10} vg/animal at post-natal day 1 [P1]) compared to PBS-injected *Cln6*^{nclf} mice. Mean ± SEM; n = 3–9 mice/treatment group. One-way ANOVA, Bonferroni correction, *p < 0.05, ****p < 0.0001. Bottom blots: probed by western blotting, delivery of the scAAV9.CB.CLN6 vector (i.c.v., P1 injection, 5×10^{10} vg/animal) shows a marked increase in hCLN6 protein expression (25 kDa) in the cerebral cortex of *Cln6*^{nclf} mice. n = 3 mice/treatment group. (B) RNAscope analysis confirms widespread transduction of *hCLN6* mRNA in the brain of 6- and 18-month-old scAAV9.CB.CLN6-injected *Cln6*^{nclf} mice (i.c.v., P1 injection, 5×10^{10} vg/animal), specifically in Batten disease-relevant regions. Scale bars, 50 μm. (C) Immunohistochemistry using anti-hCLN6 antibodies shows protein expression in various brain regions of 6- and 18-month-old scAAV9.CB.CLN6-injected *Cln6*^{nclf} mice (i.c.v., P1 injection, 5×10^{10} vg/animal), specifically in Batten disease-relevant regions. Scale bars, 50 μm.

the storage material is mitochondrial ATP synthase subunit C.[4] At 2, 6, and 18 months of age post-injection, *Cln6*^{nclf} mice treated with scAAV9.CB.CLN6 (i.c.v., P1, 5×10^{10} vg/animal) had significantly reduced levels of ATP synthase subunit C accumulation within the VPM/VPL and somatosensory cortex of the brain, compared to control *Cln6*^{nclf} mice injected with PBS (Figure 2B; Figure S2C).

Apart from the accumulation of storage material, other histological markers of disease progression include reactive gliosis, which occurs later in disease progression, and the reduction in dendritic spine density.[20] At 6 and 18 months of age post-injection, *Cln6*^{nclf} mice treated with scAAV9.CB.CLN6 (i.c.v., P1, 5×10^{10} vg/animal) had significantly reduced astrocyte activation (glial fibrillary acidic protein [GFAP]) and microgliosis (CD68) in the VPM/VPL and somatosensory cortex as compared to moribund PBS-treated *Cln6*^{nclf} mice (Figures 3A and 3B; the insets in Figure 3B show the morphology of microglia). To examine whether delivery of scAAV9.CB.CLN6 affected specific neuronal degeneration in *Cln6* mutant mice, we examined dendritic spine density using classic Golgi-Cox impregnation techniques. Importantly, a single injection of scAAV9.CB.CLN6 (i.c.v., P1, 5×10^{10} vg/animal) prevented early dendritic spine loss in 2-month-old *Cln6*^{nclf} mice (Figure 4A).

As hCLN6 expression via AAV9 prevented many of the classic Batten disease pathologies at several time points and considering CLN6 is a transmembrane protein, we were interested in determining whether hCLN6 expression prevented these pathologies in only the cells that were transduced or if neighboring cells were also protected. When examining individual cell burden for storage material, we found that cortical cells from 18-month-old scAAV9.CB.CLN6-treated mice (i.c.v., P1, 5×10^{10} vg/animal) were only protected from storage material burden if hCLN6 was present in that particular cell (Figure 4B). As such, while a single injection delivering scAAV9.CB.CLN6 into the CSF at P1 can prevent many of the classic CLN6-Batten disease pathologies in the brains of *Cln6*^{nclf} mice, it appears that this effect is likely contained to the cells that are transduced upon delivery.

Sustained Expression of hCLN6 Corrects Many of the Behavioral Deficits in Cln6^{nclf} Mice

Our previous work demonstrated that the *Cln6*^{nclf} mouse model of CLN6-Batten disease recapitulates many of the motor, cognitive, and survival defects seen in humans.[20] In the current study, using the rotarod as a classic measure of motor coordination, PBS-injected *Cln6*^{nclf} mice began to show a decline in rotarod performance at 8 months of age compared to wild-type. However, the injection of *Cln6*^{nclf} mice with scAAV9.CB.CLN6 (i.c.v., P1, 5×10^{10} vg/animal) prevented this decline, an effect that lasted for the duration of the entire study period (24 months) (Figure 5A). To further study the effects of motor

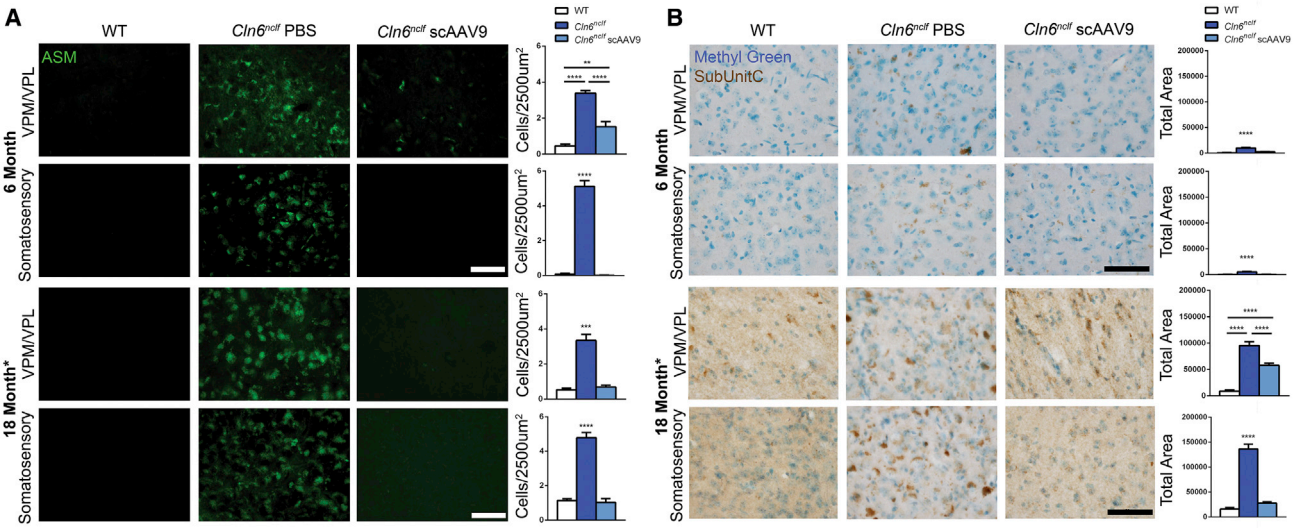

Figure 2. Sustained Expression of *hCLN6* Delays Storage Material Accumulation in *Cln6*^{nclf}-Mutant Mice

(A) A single i.c.v. injection of scAAV9.CB.CLN6 at P1 (5×10^{10} vg/animal) reduces the accumulation of autofluorescent storage material in the VPM/VPL and somatosensory cortex of 6- and 18-month *Cln6*^{nclf} mice. Graphs show the number of ASM^{+} cells/2,500 μm^2. Mean ± SEM; n = 3–10 animals/treatment group, with all images averaged to one value/animal. One-way ANOVA, Bonferroni correction, *p < 0.05, **p < 0.01, ***p < 0.001, ****p < 0.0001. Scale bar, 50 μm. (B) scAAV9.CB.CLN6 injection (i.c.v., P1 injection, 5×10^{10} vg/animal) prevents the accumulation of mitochondrial ATP synthase subunit C in the VPM/VPL and somatosensory cortex of 6- and 18-month-old *Cln6*^{nclf} mice. Brown stain represents subunit C, while blue stain represents methyl green (nuclei). Graphs show total SubC^{+} area per image field. Mean ± SEM; n = 21–72 images/treatment group, biological n = 3–10 animals/treatment group. One-way ANOVA, Bonferroni correction, *p < 0.05, **p < 0.01, ***p < 0.001, ****p < 0.0001. Scale bar, 50 μm.

coordination in detail, animals were subjected to various motor tasks (hind limb clasping, ability to lower oneself from a ledge, and gait assessment) at 12, 18, and 24 months of age, and they were assessed using a scoring matrix, with the highest score indicating the worst prognosis.[26] Compared to PBS-treated *Cln6*^{nclf} mice, mice treated with scAAV9.CB.CLN6 (i.c.v., P1, 5×10^{10} vg/animal) showed significantly lower combined scores at all time points, with a slight increase in their score only at 24 months of age (Figure 5B).

As a measure of memory and learning abilities, mice were taken through a classic Morris water maze until 24 months of age. PBS-treated *Cln6*^{nclf} mice performed poorly at the task starting at 9 months of age, indicated by their reduced ability to find the hidden platform, and treatment of *Cln6*^{nclf} mice with scAAV9.CB.CLN6 (i.c.v., P1, 5×10^{10} vg/animal) corrected this memory and learning deficit up to 12 months post-injection (Figure 5C). However, it is worth noting that the swim speeds of PBS-treated *Cln6*^{nclf} mice were significantly reduced at 11 and 12 months of age, limiting the conclusions we could draw on memory and learning abilities of untreated animals at these later time points (Figure S5A). When comparing wild-type mice to scAAV9.CB.CLN6-treated animals (i.c.v., P1, 5×10^{10} vg/animal) at later time points in the Morris water maze test, we found that even the treated mice needed more time to find the platform at 18 and 24 months, while the swim speed was the same among all test groups (Figure 5C; Figure S5A). To assess more subtle aspects of memory and learning, we also subjected mice to a water maze reversal test at 12, 18, and 24 months of age, where the platform was moved to a novel location. *Cln6*^{nclf} mice treated with scAAV9.CB.CLN6 (i.c.v., P1, 5×10^{10} vg/animal) took significantly longer to find the new platform location compared to wild-type mice in this test as well (Figure S5B). Taken together, these results indicate that a single treatment of scAAV9.CB.CLN6 prevents many of the motor declines seen in these animals, but it does not fully ward off memory and learning deficits when the mice are tested at later time points.

Single i.c.v. Injection of scAAV9.CB.CLN6 Substantially Increases the Survival of Cln6^{nclf} Mice

We have previously shown that *Cln6*^{nclf} mice have reduced survival compared to their wild-type counterparts.[20] We compared the survival of scAAV9.CB.CLN6- and PBS-injected *Cln6*^{nclf} mice with PBS-injected wild-type mice. A single i.c.v. injection of scAAV9.CB.CLN6 (5×10^{10} vg/animal) into the CSF of *Cln6*^{nclf} mice at P1 significantly increased animal survival compared to PBS-injected *Cln6*^{nclf} mice (Figure 5D). While the median survival of PBS-treated animals was 14 months, scAAV9.CB.CLN6-treated mice had a median survival of 21.5 months. This is a highly significant 65% increase in survival rate. Moreover, the survival curve of scAAV9.CB.CLN6-treated *Cln6*^{nclf} mice was not significantly different from wild-type animals.

Further, as a measure of overall health, body weight was recorded monthly. The improvement in health and survival was also underlined by the ability of scAAV9.CB.CLN6-treated mice to maintain their body weight, as no difference was observed compared to wild-type animals, while PBS-treated *Cln6*^{nclf} mice started losing weight around month 12 (Figure S5C).

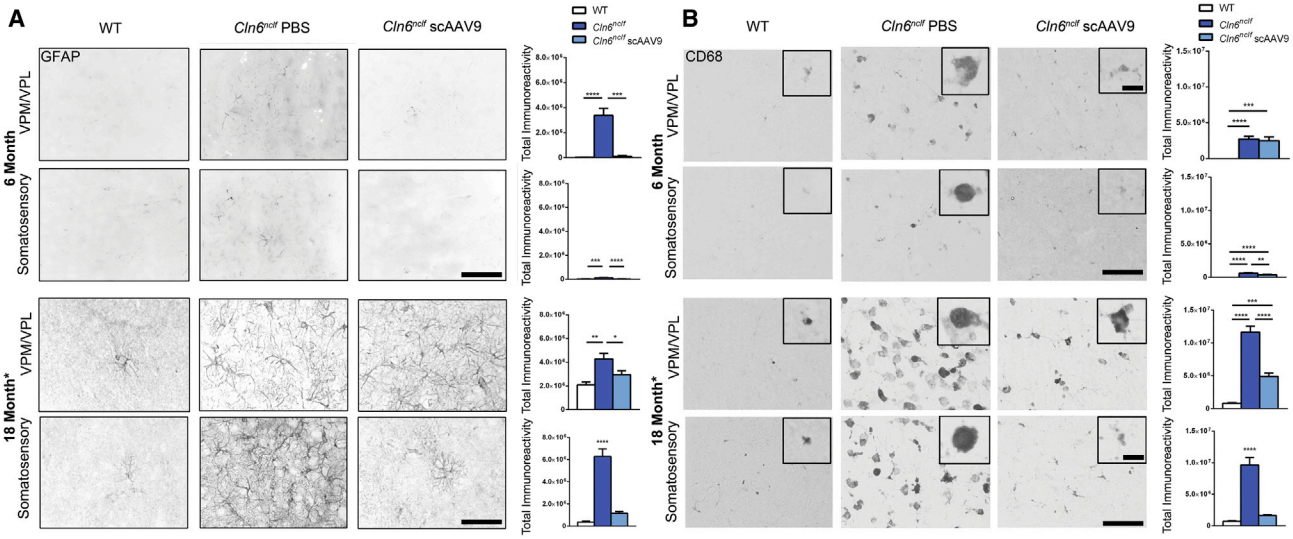

Figure 3. Sustained Expression of *hCLN6* Reduces Gliosis in *Cln6*^{ncl}-Mutant Mice

(A) scAAV9.CB.CLN6-injected *Cln6*^{ncl} mice (i.c.v., P1 injection, 5×10^{10} vg/animal) exhibit less astrogliosis (GFAP reactivity) in the VPM/VPL and somatosensory cortex at 6 and 18 months of age. Graphs show total GFAP^{+} immunoreactivity. Mean ± SEM; n = 15–44 images/treatment group, biological n = 3–10 animals/treatment group. One-way ANOVA, Bonferroni correction, *p < 0.05, **p < 0.01, ***p < 0.001, ****p < 0.0001. Scale bar, 50 μm. (B) scAAV9.CB.CLN6 injection (i.c.v., P1 injection, 5×10^{10} vg/animal) reduces microgliosis (CD68 reactivity) in the somatosensory cortex of 6-month *Cln6*^{ncl} mice and in both the VPM/VPL and somatosensory cortex of 18-month *Cln6*^{ncl} mice. Graphs show total CD68^{+} immunoreactivity. Mean ± SEM; n = 16–49 images/treatment group, biological n = 3–10 animals/treatment group. One-way ANOVA, Bonferroni correction, *p < 0.05, **p < 0.01, ***p < 0.001, ****p < 0.0001. Scale bar, 50 μm. Inset scale bar, 10 μm.

As a part of investigational new drug (IND)-enabling studies, we also performed a safety study with 172 wild-type mice treated with PBS and 223 wild-type mice treated with 5×10^{10} vg/animal scAAV9.CB.CLN6 (i.c.v., P1), and we found that scAAV9.CB.CLN6 was well tolerated up to 24 weeks with no adverse effects attributable to the virus (data not shown). Taken together, we report the longest survival extension in the *Cln6*^{nclf} mouse model to date, and the data indicate the utility of a single treatment of scAAV9.CB.CLN6 to restore both cellular and functional deficits of CLN6-Batten disease.

Lumbar Intrathecal CSF Delivery of scAAV9.CB.CLN6 in Three 4-Year-Old Non-human Primates Is Safe and Well Tolerated

To test the safety of this treatment in a large animal model more relevant to human patients, we injected three 4-year-old male cynomolgus macaques with scAAV9.CB.CLN6. The animals were sacrificed at 1, 3, or 6 months post-injection. Each individual received a single lumbar intrathecal injection, delivering the viral vector directly into the CSF at a dose of 6×10^{13} viral particles/animal. After the injection, the animals were held in a Trendelenburg position for 15 min, with head facing downward in a 45-degree angle to facilitate targeting of the brain and upper spinal cord areas, as previously demonstrated by our laboratory.[25] All subjects recovered well from the injection and did not show any abnormal behavior.

A high expression of the transgene was found throughout the brain and spinal cord of all three animals (Figures 6A and 6B). Hematology and serum chemistry were performed at up to 5 time points during the study (baseline and 1, 2, 3, and 6 months), and they did not reveal major abnormalities. In particular, no evidence of elevation in aspartate aminotransferase (AST) or alkaline phosphatase (Alk Phos) enzyme levels was found, while alanine aminotransferase (ALT) was slightly increased in one animal at 1 month post-injection (below 200 U/L) (Figure 6C). No changes were found in total protein levels, creatinine, triglycerides, glucose, or ions such as phosphorus, calcium, magnesium, or sodium levels. Extensive histopathology was performed for each animal at the time of sacrifice. No abnormalities were found in any tissue analyzed, including various brain and spinal cord regions, heart, lung, liver, spleen, kidney, small intestine, skeletal muscles (diaphragm, triceps, tibialis anterior [TA], and gastrocnemius), and gonads, except for one animal that displayed a bladder infection at the time of necropsy. Together, our data indicate that the treatment with scAAV9.CB.CLN6 was well tolerated and safe in all three animals tested.

DISCUSSION

CLN6-Batten disease is a devastating neurodegenerative disease for which there is no cure or treatment available. CLN6 is ubiquitously expressed throughout the body, and it is unclear why neurons are more vulnerable to a loss of CLN6 compared to other cell populations.[27] Identification of potential therapeutic targets has been hindered because the functions and mechanisms of action of CLN6 are largely unknown.[28,29] Mutations in the *CLN6* gene that result in CLN6-Batten disease are largely thought to be loss-of-function mutations caused by truncation of the protein and its subsequent rapid degradation.[21,30] Reintroducing a functional copy of *CLN6* using an AAV-mediated gene delivery is an attractive approach that does

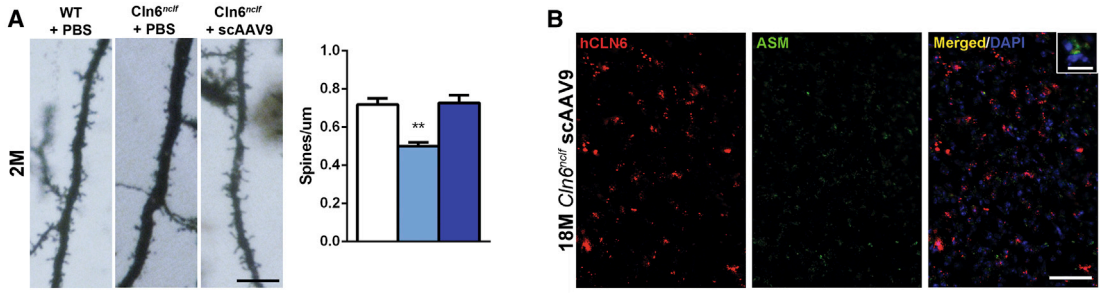

Figure 4. hCLN6 Expression Prevents Storage Material Accumulation in Individual Cells, and It Prevents Dendritic Spine Loss in Cln6-Mutant Mice

(A) Golgi impregnation of neurons and quantification of dendritic spine density, showing scAAV9.CB.CLN6 injection at P1 (i.c.v., P1 injection, 5×10^{10} vg/animal) corrects dendritic spine deficits in *Cln6*^{nclf} mice at 2 months of age. Mean ± SEM; n = 3–4 animals/treatment group, 15 neurons were counted per animal and averaged into one value per animal. One-way ANOVA, **p < 0.01. Scale bar, 10 μm. (B) Representative images from 18-month *Cln6*^{nclf} tissues show that a single i.c.v. injection of scAAV9.CB.CLN6 at P1 (5×10^{10} vg/animal) prevents ASM accumulation (green) only in the cells that express hCLN6 (red). Cells that do not express hCLN6 present with some ASM accumulation (inset). Scale bar, 50 μm. Inset scale bar, 12 μm.

not require precise knowledge of CLN6 function, and it has been explored in varying approaches in several NCLs.[31]

The successful use of AAV-mediated gene therapy is dependent upon many factors, including careful selection of the AAV serotype and its tropism, the method of administration, the animal model and its age, the amount of virus, and the promoter driving gene expression. The promoters driving gene expression should be selected based on the desired cellular targets and the levels of expression desired. In the Bosch et al.[32] study, they found that a low-expressing promoter, methyl-CpG-binding protein 2, driving *Cln3* expression resulted in better outcomes compared to a high-expressing beta-actin promoter in a mouse model of CLN3-Batten Disease. The hybrid chicken β-actin promoter was chosen for this study based on its ability to robustly drive gene expression in the CNS while being well tolerated.[22]

There are many AAV serotypes, including recombinant AAV serotypes, which differ in their tropism (reviewed in Castle et al.[33]). The AAV9 vector was chosen here for its ability to robustly target neurons and non-neuronal cells throughout the CNS.[34–36] In addition to the serotype, the timing and method of injection can influence the biodistribution of the virus. In the mouse, at P1, the tropism of the AAV9 virus targets neurons and glia equally.[37,38] After P1, the tropism of AAV9 in mice begins to shift from neurons and begins to preferentially target glia, a phenomenon that does not seem to occur in non-human primates.[23,37,39]

Studies from the Kaspar lab and others[24,25,40] have shown that both intravenous and i.c.v. administrations of AAV9 result in viral transduction throughout the CNS. However, when the Kaspar group and others[24,25,40] used scAAV9.CBA.SMN to treat spinal muscular atrophy in SMNΔ7 mice, intravenous (3.3e14 vg/kg at P1) administration required ten times more virus than an i.c.v. (3.3e13 vg/kg) delivery to achieve rescue of the spinal muscular atrophy (SMA) phenotype. Using the minimum amount of virus to achieve efficacy in treatment of the disease is important, because several studies have shown that using too much virus can result in toxicity.[41,42] Using the i.c.v. delivery, we were able to limit our viral injection to 5×10^{10} vg/animal, and, by injecting directly into the CSF, more of the virus was retained in the CNS, reducing the exposure of organ systems outside the CNS to the virus itself.[43] Our safety studies included 395 mice and three non-human primates, and we found that scAAV9.CB.CLN6 was well tolerated and safe in both mammalian model systems.

In this study, we demonstrate that a single i.c.v.-mediated injection of scAAV9.CB.CLN6 (5×10^{10} vg/animal) into the CSF of P1 mice was sufficient to induce stable, robust expression of hCLN6 protein throughout the CNS for up to 18 months. While it is tempting to question the clinical relevance of this approach, particularly the timing of treatment, we believe that the efficacy of this treatment will spur earlier diagnostic testing in the future (i.e., prenatal screenings), thereby making our early treatment protocol extremely relevant. Further, we anticipate the ongoing clinical trial to show slowed or halted disease progression in symptomatic patients treated with this vector, which may markedly improve their quality of life, even if not fully curative.

While we demonstrate robust mRNA and protein expressions of hCLN6, there are certainly inconsistencies across gene and protein expression, time points, and brain regions. Unfortunately, we cannot accurately compare RNA and protein expressions across time points, as each cohort of mice was immunolabeled in separate batches. However, we do believe that any differences between the time points are likely related to individual animal variability. Differences between mRNA and protein expressions are similarly hard to determine, though there are many possible explanations, including animal and injection variability, conditions of RNAscope incubation versus conditions of immunolabeling conditions, and the possibility of our RNAscope probes/hCLN6 antibody only partially detecting actual signal. As such, we cannot definitively conclude on the precise stability of hCLN6 expression, though this may be the subject of future study.

Additionally, the injection of scAAV9.CB.CLN6 in *Cln6*^{nclf} mice reduced many of the pathological hallmarks of CLN6-Batten disease and corrected many of the behavioral deficits characteristic of this

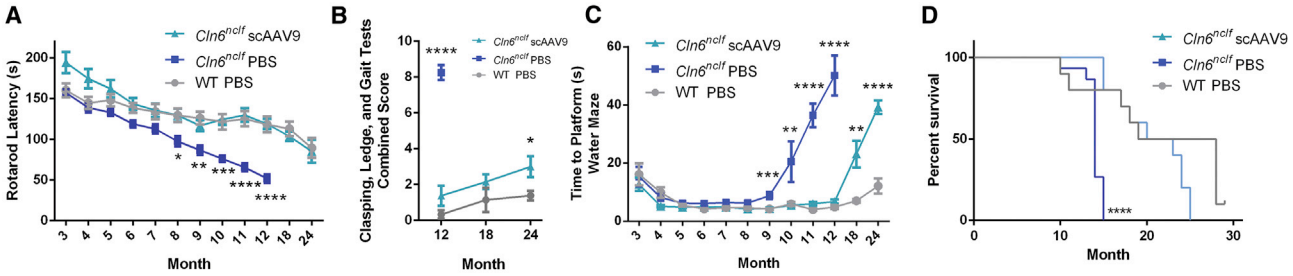

Figure 5. Sustained Expression of *hCLN6* Rescues the Motor, Memory, Learning, and Survival Deficits of *Cln6*^{nclf} Mice

(A) A single i.c.v. injection of scAAV9.CB.CLN6 at P1 (5×10^{10} vg/animal) prevents rotarod deficits from 8 to 24 months of age in *Cln6*^{nclf} mice. Mean ± SEM; n = 6–24 animals/treatment group. One-way ANOVA with Bonferroni correction or unpaired t test used where appropriate. (B) scAAV9.CB.CLN6 injection (i.c.v., P1 injection, 5×10^{10} vg/animal) corrects hind limb-clasping, gait, and ledge-lowering deficits in *Cln6*^{nclf} mice at 12 and 18 months of age. Mean ± SEM; n = 7–13 animals/treatment group. One-way ANOVA with Bonferroni correction or unpaired t test used where appropriate. (C) scAAV9.CB.CLN6 (i.c.v., P1 injection, 5×10^{10} vg/animal) prevents memory and learning deficits in the Morris water maze from 9 to 12 months of age in *Cln6*^{nclf} mice. Mean ± SEM; n = 5–15 animals/treatment group. One-way ANOVA with Bonferroni correction or unpaired t test used where appropriate. (D) scAAV9.CB.CLN6 injection (i.c.v., P1 injection, 5×10^{10} vg/animal) prevents early death of *Cln6*^{nclf} animals, while PBS-injected *Cln6*^{nclf} animals die by 15 months of age. See also Table S1 for a description of moribund conditions. n = 10–15 animals/treatment group. Log rank (Mantel-Cox) test, *p < 0.05, **p < 0.01, ***p < 0.001, ****p < 0.0001 for all graphs.

model, with the exception of the Morris water maze test. Importantly, Batten disease also affects visual capabilities, which we did not explore in this particular publication. It is possible that visual deficits may have played a role in scAAV9.CB.CLN6-treated mice performing poorly in the water maze task, and, as such, the ability of a single, i.c.v. injection of scAAV9.CB.CLN6 to rescue visual deficits will remain the subject of future studies. In addition to improving these behavioral deficits, the administration of scAAV9.CB.CLN6 increased the longevity of the *Cln6*^{nclf} mice. None of the *Cln6*^{nclf} PBS-injected mice survived past 15 months, whereas a single injection of scAAV9.CB.CLN6 in the *Cln6*^{nclf} mice at P1 resulted in a 225-day increase in median survival, which to our knowledge is the largest increase in survival in a Batten disease mouse model using AAV-mediated gene therapy.

Taken together, these results indicate the outstanding efficacy of a single, i.c.v. injection of scAAV9.CB.CLN6 into the CSF of P1 *Cln6*^{nclf} mice and safety of scAAV9.CB.CLN6 in both mice and primates. Based on these promising data, this gene therapy construct has moved into a phase I/II safety trial for CLN6-Batten disease patients (ClinicalTrials.gov: NCT02725580).

MATERIALS AND METHODS

Ethics Statement and Animals

Wild-type and homozygous *Cln6*-mutant mice (*Cln6*^{nclf}) on C57BL/6J backgrounds were used for all studies and were housed under identical conditions. Mice received a single i.c.v. injection of either PBS or scAAV9.CB.CLN6 (5×10^{10} vg/animal in 4-μL volume) at P1 (the day after birth), following hypothermia sedation. Animals were monitored continuously until fully recovered from sedation and daily thereafter. All animals were genotyped using previously described techniques.[20]

There were several separate cohorts of mice used throughout the study, all receiving a single i.c.v. injection of either PBS or scAAV9.CB.CLN6 (5×10^{10} vg/animal) at P1. Cohort 1 consisted of 4–5 animals per sex per treatment group, and they were used for all 2-month expression and pathology assays (qPCR, western, RNAscope, hCLN6 immunohistochemistry [IHC], Batten disease histopathology [ASM, SubC, GFAP, and CD68], and dendritic spine density). Cohort 2 consisted of 2–3 animals per sex per treatment group, and they were used for all 6-month expression and pathology assays (qPCR, western, RNAscope, hCLN6 IHC, and Batten disease histopathology [ASM, SubC, GFAP, and CD68]). Lastly, cohort 3 consisted of 10–14 animals per sex per treatment group; they were used for all behavioral assays from 3 to 24 months of age and monitored for survival. From this same cohort (cohort 3), 2 male and 2 female untreated *Cln6*^{nclf} animals were used for expression and pathology assays as they became moribund, and 3 wild-type (WT) and 3 treated *Cln6*^{nclf} animals (mixed sexes) were sacrificed at 18 months of age to compare to the moribund *Cln6*^{nclf} tissues. Assays at this endpoint included qPCR, western, RNAscope, hCLN6 IHC, and Batten disease histopathology (ASM, SubC, GFAP, and CD68). Taken together, assays from each time point were conducted on the same cohort of animals, and it was only the endpoint cohort that had any behavior testing before tissue was assessed for expression and pathology. Additionally, all assays were run independently on each cohort as samples became available, which limits any correlation between time points for the same assay.

All non-human primates were housed at the Mannheimer Foundation (Homestead, FL, USA), an assessment and accreditation of laboratory animal care (AAALAC)-accredited facility following the specifications recommended in The Guide for the Care and Use of Laboratory Animals (National Academy Press, Washington, DC, 1996). Each individual received a single lumbar intrathecal injection, delivering the viral vector directly into the CSF at a dose of 6×10^{13} viral particles per animal. After the injection, the animals were held in a Trendelenburg position for 15 min with head facing downward in a 45-degree angle to facilitate targeting of the brain and upper spinal cord areas, as previously demonstrated by our laboratory.[25] All subjects recovered well from the injection and did not show any abnormal behavior. For

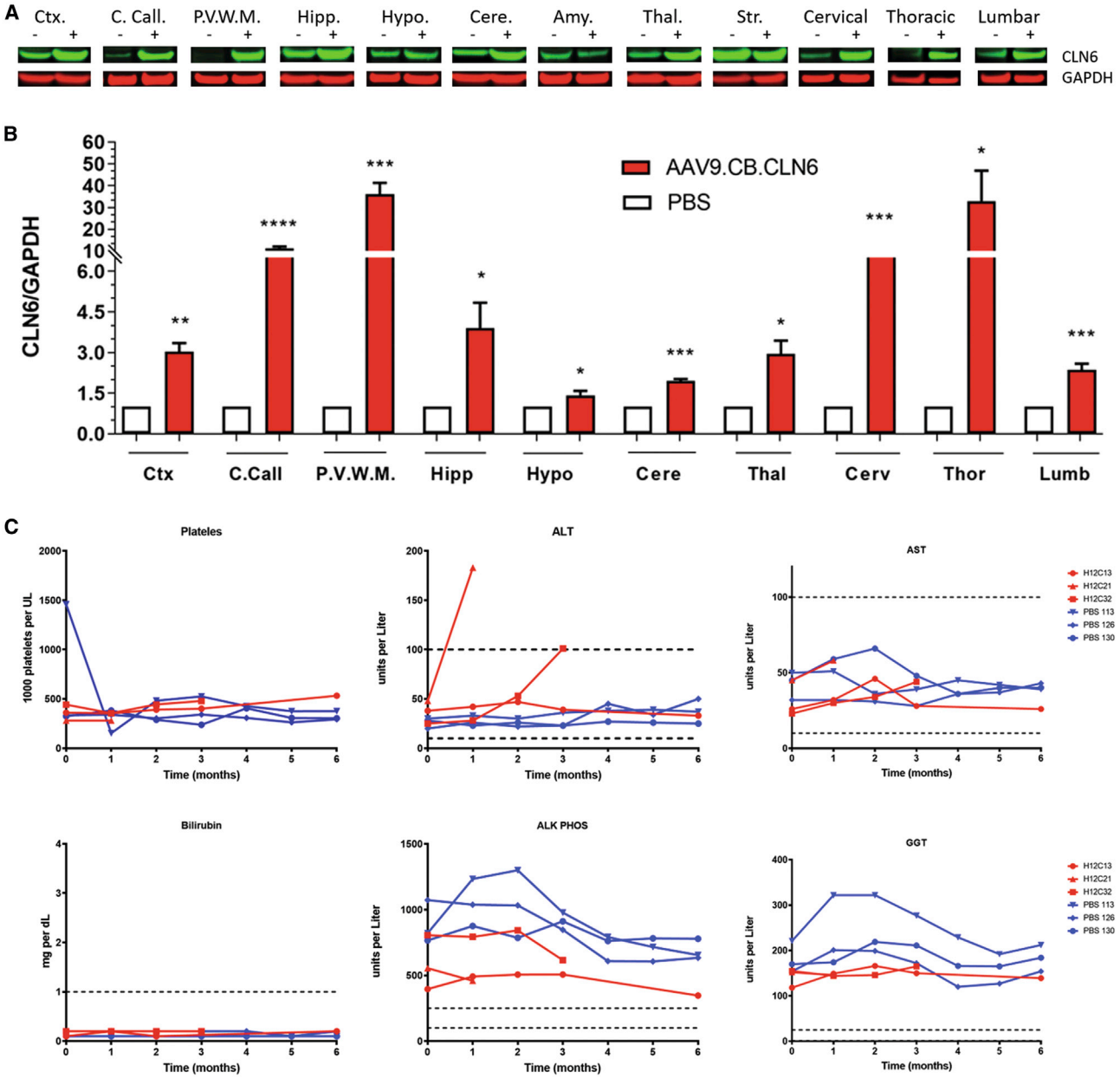

Figure 6. scAAV9.CB.CLN6 Is Highly Expressed and Well Tolerated in Non-human Primates

(A) A single lumbar intrathecal injection delivering scAAV9.CB.CLN6 into the cerebral spinal fluid (6×10^{13} viral particles/animal) induces a high expression of the transgene throughout the brain and spinal cord of non-human primates, as shown by fluorescent western blot. Blots representative of 3 animals, with "+" indicating an animal with scAAV9.CB.CLN6 treatment. Ctx., cortex; C. Call., corpus callosum; P.V.W.M., periventricular white matter; Hipp., hippocampus; Cere., cerebellum; Thal., thalamus; Cervical, cervical spinal cord; Thoracic, thoracic spinal cord; Lumbar, lumbar spinal cord. (B) Quantification of fluorescent western blots in (A). Mean ± SEM; n = 3. Unpaired Student's t test, *$p < 0.05$, **$p < 0.01$, ***$p < 0.001$, ****$p < 0.0001$. (C) Delivery of scAAV9.CB.CLN6 (single lumbar intrathecal, 6×10^{13} viral particles/animal) did not alter platelet concentration or elevate liver enzymes in the majority of non-human primates. Red data points indicate scAAV9.CB.CLN6-treated animals; blue data points indicate PBS-treated animals. ALT, alanine aminotransferase; AST, aspartate aminotransferase; Alk Phos, alkaline phosphatase; GGT, gamma-glutamyl transferase.

platelet count and liver enzyme analysis, non-human primates were bled via the femoral vein, with non-terminal bleeds extracting no more that 1% body weight. Hematology and serum chemistry were analyzed by a third party company (Antech Diagnostics).

Vector

A human CLN6 cDNA clone was obtained from OriGene (Rockville, MD). hCLN6 cDNA was further subcloned into an AAV vector under the hybrid chicken β-actin promoter and tested

in vitro and *in vivo*. The scAAV9.CB.CLN6 was produced by transient transfection procedures using a double-stranded AAV2-inverted terminal repeat (ITR)-based CB-CLN6 vector, with a plasmid encoding the Rep2Cap9 sequence, as previously described, along with an adenoviral helper plasmid pHelper (Stratagene, Santa Clara, CA) in HEK293 cells.[34] The purity and titer of the vector were assessed by silver staining and qPCR analysis.

RT-PCR

Mice were CO_2 euthanized and a lateral section of the cortical brain was collected and frozen for RNA isolation. Total RNA was extracted using a Maxwell 16 MDx instrument and the Maxwell 16 LEV simplyRNA tissue kit (Promega), according to the manufacturer's protocol. RNA quality and concentration were assayed using a BioTek Epoch Microplate Spectrophotometer, and only samples with concentrations between 200 and 1,000 ng/μL and an A260/A280 > 1.8 were used. Total RNA (1 μg) was used for reverse transcription using the Promega GoScript Reverse Transcription System (A5001) and following the manufacturer's suggested protocol. PCR was performed using 0.5 μL cDNA and 400 nM primers (*hCLN6* forward 5′-AAC GTC ATC ACG CCC TTT CT-3′, *hCLN6* reverse 5′-GAA GAG CAG GCG GTG GTT G-3′, *Gapdh* forward 5′-ACC ACA GTC CAT GCC ATC AC-3′, and *Gapdh* reverse 5′-ACC ACA GTC CAT GCC ATC AC-3′) in a 25-μL reaction using a 3-step PCR reaction for 30 cycles and an annealing temp of 60°C. The *hCLN6* RT-PCR probes had little cross-reactivity with mouse *Cln6*, as demonstrated in Figure 1A. PCR products were run on a 1% agarose gel and stained with ethidium bromide. Bands were visualized under UV light using a Gel-Doc Imager (UVP). Densitometry was performed with VisionWorks software (UVP).

In Utero Electroporation

All surgeries used sterile technique and were performed with approval from Sanford Research institutional animal care and use committee (IACUC). Briefly, dams at embryonic day (E)15.5 of pregnancy were anesthetized with 3% isoflurane, then a 1- to 2-cm abdominal midline incision was made. The uterine horns were gently pulled out to expose the pups and kept moist with sterile saline. Approximately 2 μL endotoxin-free, sterile plasmid solution was injected through the uterine tissue into a lateral cerebral ventricle of each pup using a 30G needle, followed by electroporation with five pulses of 50 V at 500-ms intervals via 3-mm diameter disc electrodes. The uterine horns were placed back into the dam, and the abdomen was remoistened. The muscle and skin layers were closed using a 6-0 silk suture with a simple interrupted pattern. Triple antibiotic ointment was applied to the incision site, and the dam was placed in a pre-warmed cage to recover from anesthesia.

CLN6 Transcript Detection Using RNAscope

Mice were CO_2 euthanized and cardiac perfused with PBS. Brains were collected and placed on a 1-mm sagittal brain block. Brains were sliced at the midline and 3 mm right of the midline. The 3-mm sagittal piece was flash frozen with −50°C isopentane and then sectioned on a cryostat at 16 μm and placed on slides. Slides were then processed according to the manufacturer's suggested protocols (ACDBio manuals 320293 and 320513). Sections were labeled with a human-specific CLN6 probe (ACDBio 452478), which consisted of 6 double Z pairs in regions of the *Cln6* gene with little homology between mouse and human *CLN6*. The *hCLN6* probes had little to no cross-reactivity with mouse *Cln6*, as demonstrated in Figure 1B (wild-type panels). Slides were fluorescently labeled with the RNAscope Fluorescent Multiplex Kit (ACDBio 320850) using their Amp 4-FL-AltB, which tagged the hCLN6 probe with a 550-nm fluorophore; slides were counterstained with DAPI to label nuclei. Tissue sections were mounted on slides under coverslips using antifade mounting media (Dako faramount, Agilent). Slides were stored in the dark before imaging.

Immunoblotting and Histopathology

Wild-type and *Cln6*^{nclf} mice were CO_2 euthanized, perfused with PBS, and tissue was either frozen or fixed with 4% paraformaldehyde (PFA). Immunoblotting was performed as previously described using anti-hCLN6 and anti-β-actin antibodies.[44,45] Rabbit polyclonal anti-hCLN6 antibody was raised against a synthetic peptide corresponding to the N-terminal amino acids 1–20 of human CLN6. The hCLN6 antibodies had little to no cross-reactivity with mouse Cln6, as demonstrated in Figure 1C. Fixed brains were sectioned on a vibratome at 50 μm (Leica VT10008). Sections were processed with standard immunofluorescence and 3,3'-diaminobenzidine (DAB)-staining protocols. The primary antibodies included anti-CD68 (AbD Serotec, MCA1957; 1:250), anti-GFAP (Dako, Z0334; 1:250), and anti-ATP synthase subunit C (Abcam, ab181243; 1:500). The secondary antibodies included anti-rat and anti-rabbit biotinylated (Vector Labs, BA-9400; 1:2,000) and Alexa Fluor fluorescent secondaries (1:1,500).

For the hCLN6 immunolabeling, 16-μm fixed sagittal brain sections were cut on a cryostat and processed with standard immunofluorescence staining protocols. Antibodies included anti-hCLN6 (1:250) and Alexa Fluor fluorescent secondaries (1:1,500). Sections were imaged and analyzed using a Nikon 90i microscope with NIS-Elements Advanced Research software (version [v.]4.20). Images were taken in the VPM/VPL of the thalamus and layers 2 and 3 of the somatosensory cortex, with multiple images taken of multiple tissues from each animal. For autofluorescent storage material, cells were scored positive for the accumulation of storage material when more than three autofluorescent puncta were aggregated around the nucleus. Subunit C, GFAP, and CD68 immunoreactivity was quantified using a threshold analysis in NIS-Elements Advanced Research software (v.4.20).

For determining dendritic spine density, brains were processed using a standard Golgi-Cox protocol. First, tissues were incubated in 1% $HgCl_2$, 1% $K_2Cr_2O_7$, and 0.8% K_2CrO_4 solution for 14 days. Brains were then put through a 5-day sucrose gradient, sectioned at 50 μm on a vibratome, and incubated in 50% ammonia for 30 min. Finally, brain sections were washed and incubated in 1% $Na_2S_2O_3$, washed,

mounted, and dehydrated through an ethanol and CitroSolv gradient prior to mounting on glass slides; 15 pyramidal neurons/animal were imaged from layers 5 and 6 of the cortex. Using NIS-Elements software, the length and number of dendritic spines of primary dendrites were measured using the following criteria: dendrites must be >25 μm, and spine counts must start within 35 μm of the cell body and terminate 225 μm from the cell body.

For non-human primate experiments, animals were CO_2 euthanized, perfused with PBS, and tissue was either frozen or fixed with 4% PFA. Immunoblotting was performed as previously described using anti-hCLN6 (1/500) and anti-GAPDH antibodies (Millipore, 1/5,000).[44,45] Briefly, tissue was lysed using tissue protein extraction reagent (TPER) buffer (Thermo Scientific) and complete protease inhibitor cocktail (Roche). 70 μg protein was separated by SDS-PAGE (NuPage Bis-Tris gels, Life Technologies) and transferred onto polyvinylidene fluoride (PVDF) membrane (Millipore). Membrane was blocked using Odyssey Blocking buffer (LI-COR Biosciences) and incubated with primary antibodies overnight. The following day the membrane was washed and incubated with LI-COR secondary antibodies (1/25,000), according to the manufacturer's protocols, and imaged using Odyssey CLx (LI-COR Biosciences). Rabbit polyclonal anti-hCLN6 antibody was raised against a synthetic peptide corresponding to the N-terminal amino acids 1–20 of human CLN6.

Neurobehavior Testing

Rotarod

Study groups were tested monthly (at months 3–12, 18, and 24) on a Rotamex-5 Rotarod (Columbus Instruments, Columbus, OH, USA) to assess motor abilities. The machine was set to accelerate 0.3 rpm every 2 s, with a starting speed of 0.3 rpm and a maximum speed of 36 rpm. Mice were trained for three consecutive trials, given a 30-min rest period, trained for three consecutive trials, given a second 30-min rest period, and trained for three final consecutive trials. After a 4-h rest period, mice were tested using the same paradigm as the training session. The latency time to fall from the rod was averaged from each of the nine afternoon testing sessions to produce one value per mouse.

Water Maze

Mice were tested monthly (at months 3–12, 18, and 24) in a Morris water maze apparatus to assess memory and learning deficiencies. The apparatus consisted of a 4-ft-diameter tub filled with water to about 26 in, with the goal platform submerged by 0.5 cm. The tub was aligned with four distinct visual cues at 0, 90, 180, and 270 degrees, with the platform resting in the maze at 315 degrees. Mice were first trained in a clear pool with a flagged platform. Mice were given 60 s to complete each trial, with four trials in the morning, followed by a 3-h rest period, and four additional trials in the afternoon. Mice that could not locate the platform with 50% accuracy in the time allotted were eliminated from further testing. Mice were then tested in water colored with white, non-toxic tempura paint and an unflagged platform. Mice were given 60 s to complete each trial, with four trials in the morning, followed by a 3-h rest period, followed by four additional trials in the afternoon. Mice were tested for 4 consecutive days, each day starting at a different visual cue. Mice were recorded using Any-maze video tracking software (Stoelting, Wood Dale, IL, USA); test duration and swim speed are represented as the average from 16 afternoon trials per mouse. At 12, 18, and 24 months of age, an additional 4 days of reversal testing was introduced, where the hidden platform was moved from 315 to 45 degrees.

Clasping, Ledge, and Gait Tests

Tests were performed as previously described on 12-, 18-, and 24-month-old wild-type and *Cln6*^{nclf} mice.[26] Briefly, for hind limb-clasping measurements, animals were scored on the extent to which their limbs clasped into their abdomen when held by the base of their tail (score 0–3). For ledge-lowering measurements, animals were scored on their ability to easily lower themselves from the edge of their home cage (score 0–3). For gait measurements, animals were scored on their overall ease of walking, including whether their abdomen dragged on the ground and if their limbs were splayed while walking (score 0–3).

Statistical Analysis

Statistical analyses were performed using GraphPad Prism (v.6.04) and details are noted in the figure legends. In general, one-way ANOVA was employed with a Bonferroni correction, and outliers were removed with the ROUT method (Q = 0.1%). If appropriate, an unpaired t test was used. For the survival curve analysis, the log rank (Mantel-Cox) test was used. Statistical significance was indicated as follows: $^{*}p < 0.05$, $^{**}p < 0.01$, $^{***}p < 0.001$, and $^{****}p < 0.0001$. The datasets generated during and/or analyzed during the current study are available from the corresponding author upon reasonable request.

Study Approval

All mouse studies were performed in an AAALAC-accredited facility in strict accordance with NIH guidelines, and they were approved by the Sanford Institutional Animal Care and Use Committee (U.S. Department of Agriculture [USDA] license 46-R-0009).

SUPPLEMENTAL INFORMATION

Supplemental Information can be found online at https://doi.org/10.1016/j.ymthe.2019.06.015.

AUTHOR CONTRIBUTIONS

Conceived and Designed the Experiments, J.T.C., S.L., K.A.W., D.J.T., F.R., B.K.K., K.M., and J.M.W.; Provided Reagents, S.M.H. and S.Y.L.; Executed the Experiments, J.T.C., S.L., K.A.W., D.J.T., S.S.D., T.B.J., C.N.D.-R., F.R., D.M., S.C., P.M., C.P., and K.M.; Analyzed the Data, J.T.C., S.L., K.A.W., D.J.T., T.B.J., C.N.D.-R., F.R., D.M., S.C., P.M., C.P., K.M., and J.M.W.; Contributed to the Writing of the Manuscript, J.T.C., K.A.W., D.J.T., K.M., and J.M.W.; Agreed with Manuscript Results and Conclusions, J.T.C., S.L., K.A.W., D.J.T., S.S.D., T.B.J., C.N.D.-R., F.R., D.M., S.C., P.M., C.P., S.M.H., S.Y.L., B.K.K., K.M., and J.M.W.; Jointly Developed the Structure and Arguments for the Paper, J.T.C., K.A.W., D.J.T., K.M., B.K.K., and J.M.W.;

Made Critical Revisions and Approved Final Version, J.T.C., S.L., K.A.W., D.J.T., S.S.D., T.B.J., C.N.D.-R., D.M., S.C., P.M., C.P., F.R., S.M.H., S.Y.L., B.K.K., K.M., and J.M.W. All authors reviewed and approved the final manuscript.

CONFLICTS OF INTEREST

The authors declare no competing interests.

ACKNOWLEDGMENTS

Special thanks to Steven Ortmeier, Kayla Knutson, and Rachel Laufmann for their assistance in immunohistochemistry and neurobehavior experiments. This work was supported by funding to J.M.W., K.M., and B.K.K. from the Charlotte and Gwenyth Gray Foundation and to J.M.W. from NIH R01NS082283. This work also received support from the Sanford Research Imaging Core within the Sanford Research Center for Pediatric Research (NIH P20GM103620) and the Sanford Research Molecular Pathology Core within the Sanford Research Center for Cancer Biology (NIH P20GM103548). The datasets generated during and/or analyzed during the current study are available from the corresponding author on reasonable request.

REFERENCES

1. Mole, S.E., and Cotman, S.L. (2015). Genetics of the neuronal ceroid lipofuscinoses (Batten disease). Biochim. Biophys. Acta *1852* (10 Pt B), 2237–2241.
2. Santavuori, P. (1988). Neuronal ceroid-lipofuscinoses in childhood. Brain Dev. *10*, 80–83.
3. Rider, J.A., and Rider, D.L. (1988). Batten disease: past, present, and future. Am. J. Med. Genet. Suppl. *5*, 21–26.
4. Palmer, D.N., Fearnley, I.M., Walker, J.E., Hall, N.A., Lake, B.D., Wolfe, L.S., Haltia, M., Martinus, R.D., and Jolly, R.D. (1992). Mitochondrial ATP synthase subunit c storage in the ceroid-lipofuscinoses (Batten disease). Am. J. Med. Genet. *42*, 561–567.
5. Cannelli, N., Garavaglia, B., Simonati, A., Aiello, C., Barzaghi, C., Pezzini, F., Cilio, M.R., Biancheri, R., Morbin, M., Dalla Bernardina, B., et al. (2009). Variant late infantile ceroid lipofuscinoses associated with novel mutations in CLN6. Biochem. Biophys. Res. Commun. *379*, 892–897.
6. Arsov, T., Smith, K.R., Damiano, J., Franceschetti, S., Canafoglia, L., Bromhead, C.J., Andermann, E., Vears, D.F., Cossette, P., Rajagopalan, S., et al. (2011). Kufs disease, the major adult form of neuronal ceroid lipofuscinosis, caused by mutations in CLN6. Am. J. Hum. Genet. *88*, 566–573.
7. Canafoglia, L., Gilioli, I., Invernizzi, F., Sofia, V., Fugnanesi, V., Morbin, M., Chiapparini, L., Granata, T., Binelli, S., Scaioli, V., et al. (2015). Electroclinical spectrum of the neuronal ceroid lipofuscinoses associated with CLN6 mutations. Neurology *85*, 316–324.
8. Mole, S.E., Michaux, G., Codlin, S., Wheeler, R.B., Sharp, J.D., and Cutler, D.F. (2004). CLN6, which is associated with a lysosomal storage disease, is an endoplasmic reticulum protein. Exp. Cell Res. *298*, 399–406.
9. Wheeler, R.B., Sharp, J.D., Schultz, R.A., Joslin, J.M., Williams, R.E., and Mole, S.E. (2002). The gene mutated in variant late-infantile neuronal ceroid lipofuscinosis (CLN6) and in nclf mutant mice encodes a novel predicted transmembrane protein. Am. J. Hum. Genet. *70*, 537–542.
10. Heine, C., Koch, B., Storch, S., Kohlschütter, A., Palmer, D.N., and Braulke, T. (2004). Defective endoplasmic reticulum-resident membrane protein CLN6 affects lysosomal degradation of endocytosed arylsulfatase A. J. Biol. Chem. *279*, 22347–22352.
11. Benedict, J.W., Getty, A.L., Wishart, T.M., Gillingwater, T.H., and Pearce, D.A. (2009). Protein product of CLN6 gene responsible for variant late-onset infantile neuronal ceroid lipofuscinosis interacts with CRMP-2. J. Neurosci. Res. *87*, 2157–2166.
12. Getty, A.L., Benedict, J.W., and Pearce, D.A. (2011). A novel interaction of CLN3 with nonmuscle myosin-IIB and defects in cell motility of Cln3(-/-) cells. Exp. Cell Res. *317*, 51–69.
13. Warrier, V., Vieira, M., and Mole, S.E. (2013). Genetic basis and phenotypic correlations of the neuronal ceroid lipofusinoses. Biochim. Biophys. Acta *1832*, 1827–1830.
14. Kurze, A.K., Galliciotti, G., Heine, C., Mole, S.E., Quitsch, A., and Braulke, T. (2010). Pathogenic mutations cause rapid degradation of lysosomal storage disease-related membrane protein CLN6. Hum. Mutat. *31*, E1163–E1174.
15. Bond, M., Holthaus, S.M., Tammen, I., Tear, G., and Russell, C. (2013). Use of model organisms for the study of neuronal ceroid lipofuscinosis. Biochim. Biophys. Acta *1832*, 1842–1865.
16. Broom, M.F., Zhou, C., Broom, J.E., Barwell, K.J., Jolly, R.D., and Hill, D.F. (1998). Ovine neuronal ceroid lipofuscinosis: a large animal model syntenic with the human neuronal ceroid lipofuscinosis variant CLN6. J. Med. Genet. *35*, 717–721.
17. Tammen, I., Cook, R.W., Nicholas, F.W., and Raadsma, H.W. (2001). Neuronal ceroid lipofuscinosis in Australian Merino sheep: a new animal model. Eur. J. Paediatr. Neurol. *5* (*Suppl 1*), 37–41.
18. Katz, M.L., Farias, F.H., Sanders, D.N., Zeng, R., Khan, S., Johnson, G.S., and O'Brien, D.P. (2011). A missense mutation in canine CLN6 in an Australian shepherd with neuronal ceroid lipofuscinosis. J. Biomed. Biotechnol. *2011*, 198042.
19. Bronson, R.T., Donahue, L.R., Johnson, K.R., Tanner, A., Lane, P.W., and Faust, J.R. (1998). Neuronal ceroid lipofuscinosis (nclf), a new disorder of the mouse linked to chromosome 9. Am. J. Med. Genet. *77*, 289–297.
20. Morgan, J.P., Magee, H., Wong, A., Nelson, T., Koch, B., Cooper, J.D., and Weimer, J.M. (2013). A murine model of variant late infantile ceroid lipofuscinosis recapitulates behavioral and pathological phenotypes of human disease. PLoS ONE *8*, e78694.
21. Gao, H., Boustany, R.M., Espinola, J.A., Cotman, S.L., Srinidhi, L., Antonellis, K.A., Gillis, T., Qin, X., Liu, S., Donahue, L.R., et al. (2002). Mutations in a novel CLN6-encoded transmembrane protein cause variant neuronal ceroid lipofuscinosis in man and mouse. Am. J. Hum. Genet. *70*, 324–335.
22. Mendell, J.R., Al-Zaidy, S., Shell, R., Arnold, W.D., Rodino-Klapac, L.R., Prior, T.W., Lowes, L., Alfano, L., Berry, K., Church, K., et al. (2017). Single-Dose Gene-Replacement Therapy for Spinal Muscular Atrophy. N. Engl. J. Med. *377*, 1713–1722.
23. Foust, K.D., Salazar, D.L., Likhite, S., Ferraiuolo, L., Ditsworth, D., Ilieva, H., Meyer, K., Schmelzer, L., Braun, L., Cleveland, D.W., and Kaspar, B.K. (2013). Therapeutic AAV9-mediated suppression of mutant SOD1 slows disease progression and extends survival in models of inherited ALS. Mol. Ther. *21*, 2148–2159.
24. Foust, K.D., Wang, X., McGovern, V.L., Braun, L., Bevan, A.K., Haidet, A.M., Le, T.T., Morales, P.R., Rich, M.M., Burghes, A.H., and Kaspar, B.K. (2010). Rescue of the spinal muscular atrophy phenotype in a mouse model by early postnatal delivery of SMN. Nat. Biotechnol. *28*, 271–274.
25. Meyer, K., Ferraiuolo, L., Schmelzer, L., Braun, L., McGovern, V., Likhite, S., Michels, O., Govoni, A., Fitzgerald, J., Morales, P., et al. (2015). Improving single injection CSF delivery of AAV9-mediated gene therapy for SMA: a dose-response study in mice and nonhuman primates. Mol. Ther. *23*, 477–487.
26. Guyenet, S.J., Furrer, S.A., Damian, V.M., Baughan, T.D., La Spada, A.R., and Garden, G.A. (2010). A simple composite phenotype scoring system for evaluating mouse models of cerebellar ataxia. J. Vis. Exp. (39), 1787.
27. Uhlén, M., Fagerberg, L., Hallström, B.M., Lindskog, C., Oksvold, P., Mardinoglu, A., Sivertsson, Å., Kampf, C., Sjöstedt, E., Asplund, A., et al. (2015). Proteomics. Tissue-based map of the human proteome. Science *347*, 1260419.
28. Kollmann, K., Uusi-Rauva, K., Scifo, E., Tyynelä, J., Jalanko, A., and Braulke, T. (2013). Cell biology and function of neuronal ceroid lipofuscinosis-related proteins. Biochim. Biophys. Acta *1832*, 1866–1881.
29. Kyttälä, A., Lahtinen, U., Braulke, T., and Hofmann, S.L. (2006). Functional biology of the neuronal ceroid lipofuscinoses (NCL) proteins. Biochim. Biophys. Acta *1762*, 920–933.
30. Oresic, K., Mueller, B., and Tortorella, D. (2009). Cln6 mutants associated with neuronal ceroid lipofuscinosis are degraded in a proteasome-dependent manner. Biosci. Rep. *29*, 173–181.

31. Johnson, T.B., Cain, J.T., White, K.A., Ramirez-Montealegre, D., Pearce, D.A., and Weimer, J.M. (2019). Therapeutic landscape for Batten disease: current treatments and future prospects. Nat. Rev. Neurol. *15*, 161–178.

32. Bosch, M.E., Aldrich, A., Fallet, R., Odvody, J., Burkovetskaya, M., Schuberth, K., Fitzgerald, J.A., Foust, K.D., and Kielian, T. (2016). Self-Complementary AAV9 Gene Delivery Partially Corrects Pathology Associated with Juvenile Neuronal Ceroid Lipofuscinosis (CLN3). J. Neurosci. *36*, 9669–9682.

33. Castle, M.J., Turunen, H.T., Vandenberghe, L.H., and Wolfe, J.H. (2016). Controlling AAV Tropism in the Nervous System with Natural and Engineered Capsids. Methods Mol. Biol. *1382*, 133–149.

34. Foust, K.D., Nurre, E., Montgomery, C.L., Hernandez, A., Chan, C.M., and Kaspar, B.K. (2009). Intravascular AAV9 preferentially targets neonatal neurons and adult astrocytes. Nat. Biotechnol. *27*, 59–65.

35. Gray, S.J., Matagne, V., Bachaboina, L., Yadav, S., Ojeda, S.R., and Samulski, R.J. (2011). Preclinical differences of intravascular AAV9 delivery to neurons and glia: a comparative study of adult mice and nonhuman primates. Mol. Ther. *19*, 1058–1069.

36. McLean, J.R., Smith, G.A., Rocha, E.M., Hayes, M.A., Beagan, J.A., Hallett, P.J., and Isacson, O. (2014). Widespread neuron-specific transgene expression in brain and spinal cord following synapsin promoter-driven AAV9 neonatal intracerebroventricular injection. Neurosci. Lett. *576*, 73–78.

37. Schuster, D.J., Dykstra, J.A., Riedl, M.S., Kitto, K.F., Belur, L.R., McIvor, R.S., Elde, R.P., Fairbanks, C.A., and Vulchanova, L. (2014). Biodistribution of adeno-associated virus serotype 9 (AAV9) vector after intrathecal and intravenous delivery in mouse. Front. Neuroanat. *8*, 42.

38. Chakrabarty, P., Rosario, A., Cruz, P., Siemienski, Z., Ceballos-Diaz, C., Crosby, K., Jansen, K., Borchelt, D.R., Kim, J.Y., Jankowsky, J.L., et al. (2013). Capsid serotype and timing of injection determines AAV transduction in the neonatal mice brain. PLoS ONE *8*, e67680.

39. Green, F., Samaranch, L., Zhang, H.S., Manning-Bog, A., Meyer, K., Forsayeth, J., and Bankiewicz, K.S. (2016). Axonal transport of AAV9 in nonhuman primate brain. Gene Ther. *23*, 520–526.

40. Saraiva, J., Nobre, R.J., and Pereira de Almeida, L. (2016). Gene therapy for the CNS using AAVs: The impact of systemic delivery by AAV9. J. Control. Release *241*, 94–109.

41. Hinderer, C., Bell, P., Louboutin, J.P., Zhu, Y., Yu, H., Lin, G., Choa, R., Gurda, B.L., Bagel, J., O'Donnell, P., et al. (2015). Neonatal Systemic AAV Induces Tolerance to CNS Gene Therapy in MPS I Dogs and Nonhuman Primates. Mol. Ther. *23*, 1298–1307.

42. Hinderer, C., Katz, N., Buza, E.L., Dyer, C., Goode, T., Bell, P., Richman, L.K., and Wilson, J.M. (2018). Severe Toxicity in Nonhuman Primates and Piglets Following High-Dose Intravenous Administration of an Adeno-Associated Virus Vector Expressing Human SMN. Hum. Gene Ther. *29*, 285–298.

43. Armbruster, N., Lattanzi, A., Jeavons, M., Van Wittenberghe, L., Gjata, B., Marais, T., Martin, S., Vignaud, A., Voit, T., Mavilio, F., et al. (2016). Efficacy and biodistribution analysis of intracerebroventricular administration of an optimized scAAV9-SMN1 vector in a mouse model of spinal muscular atrophy. Mol. Ther. Methods Clin. Dev. *3*, 16060.

44. Weimer, J.M., Benedict, J.W., Elshatory, Y.M., Short, D.W., Ramirez-Montealegre, D., Ryan, D.A., Alexander, N.A., Federoff, H.J., Cooper, J.D., and Pearce, D.A. (2007). Alterations in striatal dopamine catabolism precede loss of substantia nigra neurons in a mouse model of juvenile neuronal ceroid lipofuscinosis. Brain Res. *1162*, 98–112.

45. Weimer, J.M., Benedict, J.W., Getty, A.L., Pontikis, C.C., Lim, M.J., Cooper, J.D., and Pearce, D.A. (2009). Cerebellar defects in a mouse model of juvenile neuronal ceroid lipofuscinosis. Brain Res. *1266*, 93–107.